ACCURATE FAULT LOCATION ALGORITHM FOR SERIES COMPENSATED LINES USING TWO-TERMINAL UNSYNCHRONIZED MEASUREMENTS AND HYDRO-QUEBEC'S FIELD EXPERIENCE

Claude Fecteau
IREQ
Research Institute of Hydro-Québec

HYDRO-QUEBEC

Presented to the

33rd Annual
Western Protective Relay Conference
Spokane, Washington
October 17-19, 2006

ACCURATE FAULT LOCATION ALGORITHM FOR SERIES COMPENSATED LINES USING TWO-TERMINAL UNSYNCHRONIZED MEASUREMENTS AND HYDRO-QUEBEC'S FIELD EXPERIENCE

Claude Fecteau

Research Institute of Hydro-Québec (IREQ)

Abstract: *This paper presents an accurate phasor-based fault location algorithm for series compensated lines. This particular problem is recognized as being an especially difficult one owing to the capacitors and their related protection (MOV, spark gap and/or bypass breaker). Phasor-based methods are very attractive to utilities because common multi-purpose Digital Fault Recorders (DFRs) and digital relays with oscillography function can be used. The proposed algorithm uses unsynchronized voltage and current measurements from both ends of the line and a method is given to correct the synchronization error using the prefault data. Thus, Phasor Measurement Units (PMUs) which use high precision clock from the Global Positioning System (GPS) for instance are not required. The algorithm is insensitive to the fault resistance and no assumption is made on external parameters such as the source impedances or the current distribution factors. It can be applied to transposed or untransposed lines, non homogeneous lines or systems, and it compensates for the mutual coupling between parallel lines if present. The algorithm also takes into account the shunt admittance of the line using a distributed parameter line model. Therefore, it is well suited even for the longest lines, which are naturally the best candidates for series compensation. Most interestingly, the modeling of the capacitor bank is not required, whether using Fixed Series Capacitor (FSC) or Thyristor Controlled Series Capacitor (TCSC). The paper describes how the new algorithm is integrated into the fully automated fault location system that has been developed at Hydro-Québec. The paper also presents some innovative integrity checks that are performed to detect crude measurement and line parameter errors. Many years of field experience are shared discussing real faults that occurred on Hydro-Québec's transmission lines.*

Contact information: fecteau.claude@ireq.ca
IREQ, 1800 boul. Lionel-Boulet, Varennes, Québec, Canada, J3X 1S1

1. INTRODUCTION

The availability of reliable electric power is of utmost importance to modern nation economy. The major blackout that has affected 50 million people in Northeast America on August 14, 2003, is estimated to have cost between $4 billion and $10 billion in United States only [1]. Such an event dramatically demonstrates the possible outcome of transmission line faults that force line openings at untimely moments and other examples abound in recent history of major blackouts [1], [2]. Fault location for transmission lines is highly desirable to speed up the searches of permanent faults. Fast repair can be critical when the lines are congested during peak periods. Fault location also helps identify the weak spots responsible for recurrent transient faults caused by trees, damaged insulators or galloping conductors for instance. The location of these faults may otherwise remain unknown until they degenerate into permanent faults. Every fault occurring in a power system also stresses the equipment and create voltage sags that deteriorate the power quality. The probability of experiencing transmission line fault increases with the length of the line and patrolling longer lines is also more time consuming. Consequently, fault location in these cases is even more beneficial.

Phasor-based fault location methods that use the fundamental frequency component of the voltages and currents present a high interest to utilities because oscillographic data obtained from common DFRs (Digital Fault Recorders), digital protective relays and other Intelligent Electronic Devices (IEDs) can be used. Fault location can thus be provided as a software function which uses already installed equipments. This is in contrast with travelling-wave based methods which require dedicated equipment for the detection and the precise timing of the wavefronts. Although such fault locators are known to provide very good precision in many circumstances (± 1 tower), the effectiveness of the method deteriorates for resistive faults because the wavefronts that are propagated are more attenuated and distorted.

Phasor-based methods can be classified as *one-terminal*, *two-terminal* or *multi-terminal*. One-terminal methods have inherent limitations that are summarized in section 2. These limitations are notably related to remote-end infeed and series compensation. A brief review of some two-terminal methods that overcome the remote-end infeed error for uncompensated lines is presented in section 3. Regarding series compensation, this proven technology applies principally on long EHV transmission lines to increase their transfer capacity while maintaining stability. Series compensated lines are recognized as setting an especially difficult problem to one- and two-terminal fault location methods owing to the capacitors and their related protection (MOV, spark gap and bypass breaker). A new phasor-based two-terminal fault location algorithm that provides an exact steady-state solution to this problem is described in section 4. A method to correct the synchronization error using the prefault data is also described. The implementation of the algorithm into a fully automated fault location system is described in section 5 and field experience on Hydro-Québec's transmission lines is also reported.

2. LIMITATIONS OF ONE-TERMINAL FAULT LOCATION ALGORITHMS

2.1 Basic Reactance Algorithm Principle

Most one-terminal phasor-based fault location methods are modified versions of the simple reactance algorithm. For explaining the principle, a one-line diagram of a faulted three phase transmission line is shown at Figure 1.

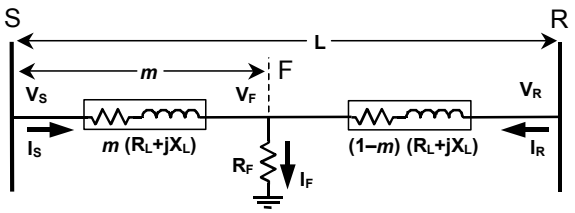

Figure 1: One-line diagram of a three phase faulted transmission line

The line of length L is connecting a bus at substation S to another bus at substation R. The total series impedance of the line is $Z_L = R_L + j\,X_L$ and the shunt admittance is neglected for simplification. The energy sources of the electrical system can be represented by Thevenin equivalents connected behind each terminal (not shown). All voltages and currents are phasors representing the fundamental frequency component of their respective time-domain signals. One-terminal algorithms are making use of the local voltage V_S and current I_S to estimate the distance m of the fault from terminal S (m is expressed in per unit for convenience in this demonstration). The fault is represented by a pure resistance R_F, assuming that the voltage at the fault point is in phase with the total fault current I_F [3].

Single Phase Case

The basic reactance algorithm principle is explained by assuming the circuit at Figure 1 is single phase at first. Applying the Kirchoff's Voltage Law (KVL), the voltage drop from terminal S is written as follows:

$$V_S = m\cdot\left(R_L + j\cdot X_L\right)\cdot I_S + R_F\cdot I_F \qquad (1)$$

The total fault current I_F is equal to the sum of the contributions from both ends:

$$I_F = I_S + I_R \qquad (2)$$

Substituting (2) in (1) and dividing both sides by I_S results in:

$$\frac{V_S}{I_S} = m\cdot\left(R_L + j\cdot X_L\right) + R_F\cdot\left(\frac{I_S + I_R}{I_S}\right) \qquad (3)$$

If the remote current I_R can be neglected relatively to the measured current I_S, then Equation (3) is reduced to a complex equation with two unknowns m and R_F:

$$Z_{app} = \frac{V_S}{I_S} = m\cdot\left(R_L + j\cdot X_L\right) + R_F \qquad (4)$$

The ratio on the left hand side represents the apparent impedance seen from terminal S. Taking the imaginary part of both sides, where the reactance algorithm name comes from, the resistive terms get eliminated:

$$imag\left\{\frac{V_S}{I_S}\right\} = m\cdot X_L \qquad (5)$$

The sought distance is then simply obtained by isolating m:

$$m = \frac{imag\left\{\frac{V_S}{I_S}\right\}}{X_L} \qquad (6)$$

It is also interesting to evaluate the fault resistance because it can provide an indication about the nature of the fault. Once m is obtained then R_F can be isolated in (4):

$$R_F = real\left\{\frac{V_S}{I_S}\right\} - m\cdot R_L \qquad (7)$$

Three Phase Case

For a three-phase system, the mutual effect between phases a, b and c must be taken into account, which lead to a specific equation for phase-to-ground faults and multi-phase

faults (phase-to-phase, double phase-to-ground and 3-phase) [3]. For a phase-a-to-ground fault for instance, the current I_S in Equation (6) is replaced by a compensated current I_{Sa}' as shown in Equation (8). For multi-phase faults involving phases b and c for example, the sought distance is given by Equation (9).

Phase-a-to-ground fault

$$m = \frac{imag\left\{\frac{V_{Sa}}{I_{Sa}'}\right\}}{X_{L1}} \quad (8)$$

where:

$$I_{Sa}' = I_{Sa} + \left(\frac{Z_{L0} - Z_{L1}}{Z_{L1}}\right) \cdot I_0 + \sum_{i=1}^{N}\left(\frac{Z_{m0i}}{Z_{L1}} \cdot I_{0\,paral\_i}\right)$$

$Z_{L0} = R_{L0} + j\,X_{L0}$ = zero sequence line impedance
$Z_{L1} = R_{L1} + j\,X_{L1}$ = positive sequence line impedance
I_0 = zero sequence current of faulted line
N = number of parallel lines
Z_{m0i} = zero sequence mutual impedance between parallel line i
$I_{0\,paral\_i}$ = zero sequence current of parallel line i

Phase-b-c, Phase-b-c-ground and 3-phase fault

$$m = \frac{imag\left\{\frac{V_{Sbc}}{I_{Sbc}}\right\}}{X_{L1}} \quad (9)$$

where: $V_{Sbc} = V_{Sb} - V_{Sc}$, $I_{Sbc} = I_{Sb} - I_{Sc}$

Similar equations are obtained when other phases are involved by permuting the indices. A faulted phase selection algorithm must be applied first to select the proper equation and signals.

Influence of zero sequence impedance and parallel lines

It can be noticed that the phase-to-ground fault equation is dependent on the zero sequence impedance of the line Z_{L0}, which is less accurate in practice than the positive sequence impedance Z_{L1}, because it depends in turn on approximate knowledge of the soil resistivity. Another possible source of error specific to phase-to-ground faults comes from the zero sequence mutual coupling between parallel lines. It is possible however to take into account this effect by adding the last term to the compensated current in Equation (8), provided that the residual currents from the parallel lines are available. If this effect is not compensated, the distance is over-estimated for zero sequence currents in parallel lines flowing in the same direction and under-estimated if they are flowing in opposite directions. The effect of zero sequence mutual coupling is highest for lines that are paralleled at close spacing such as double-circuit lines. Moreover, it is more probable to have high resistance fault for phase-to-ground fault than multi-phase fault and this noting can induce another error when remote-end infeed is present as explained next.

2.2 Effect of Remote-End Infeed

It was assumed that the remote-end current was negligible in order to derive Equation (4) above. That assumption is perfectly met if the circuit breaker at terminal *R* is open for instance, leading no algorithmic error in Equations (6) and (7). The estimation thus attains the best accuracy for the particular case of switching onto fault at line energization or reclosing. If the remote breaker is closed however, the remote current may introduce an error. Considering the single-phase case once again simplifies the error analysis which follows.

Equation (3) is rewritten to evaluate the error term:

$$Z_{app} = \frac{V_S}{I_S} = m \cdot \left(R_L + j \cdot X_L\right) + R_F + R_F \cdot \left(\frac{I_R}{I_S}\right) \quad (10)$$

Figure 2 illustrates Equation (10) graphically on the R-X diagram.

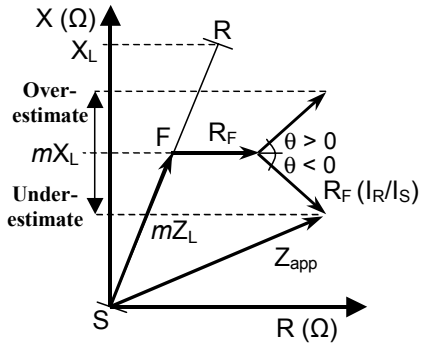

Fig. 2: Graphical error interpretation

When applying Equation (6) to (8) now provides the result:

$$\frac{imag\left\{\frac{V_S}{I_S}\right\}}{X_L} = m + \frac{R_F}{X_L} \cdot \frac{|I_R|}{|I_S|} \cdot \sin(\theta) \quad (11)$$

where: θ is the angle of I_R relative to I_S.

It can be observed that the result includes the following error term:

$$m\_error\ (p.u.) = \frac{R_F}{X_L} \cdot \frac{|I_R|}{|I_S|} \cdot \sin(\theta) \qquad (12)$$

Analysing this term leads to the following conclusions:

- Error is proportional to the fault resistance R_F
- Error is proportional to the ratio $|I_R|/|I_S|$ (error is worst for a fault at far end)
- Error increases as the angle θ between I_R and I_S increases (for $-90° < \theta < 90°$)
- Error is positive or negative depending on whether I_R is leading or lagging I_S
- Error is nil if R_F, I_R or θ is nil (I_R and I_S are in phase)
- Error has no upper boundary

It is also interesting to examine the error of the fault resistance estimate. Taking the real part of both sides of Equation (10) and applying Equation (7) leads to:

$$real\left\{\frac{V_S}{I_S}\right\} - m \cdot R_L = R_F \left(1 + \frac{|I_R|}{|I_S|} \cdot \cos(\theta)\right) \qquad (13)$$

The error term is thus written in per unit as follows:

$$R_F\_error\ (p.u.) = \frac{|I_R|}{|I_S|} \cdot \cos(\theta) \qquad (14)$$

Analysing this term leads to the following conclusions regarding the estimated fault resistance R_F:

- Error is proportional to the ratio $|I_R|/|I_S|$ (error is worst for a fault at far end)
- Fault resistance R_F is always over-estimated (for $-90° < \theta < 90°$)

Many variants of the reactance algorithm have been proposed to minimize the fault location error term. If the line is supplying loads only, then it is possible to account for the remote-end current provided that a load model is available [4]. If energy sources contribute to the fault from terminal *R*, a distant resistive fault may lead to unacceptable error when I_S and I_R and not in phase according to Equation (12). The Takagi algorithm uses the prefault loadflow to compensate partially for the angle θ between I_S and I_R [5]. Other algorithms use external parameters such as the source impedances, current distribution factors or various compensation methods to reduce the error term [6], [7]. However, these solutions are difficult to implement from a practical point of view because the additional parameters that are required are dependent on the network configuration, which is changing during normal operation.

Shunt capacitance of long EHV transmission lines

Equations presented until now consider a lumped R-L model of the line known as the *short line approximation* [8]. To obtain best fault location accuracy for long EHV transmission lines however, the long line model should be used because it takes into account the distributed nature of the shunt capacitance [10], [11]. Long line models are considered in section 3 and 4 when discussing two-terminal fault location algorithms.

2.3 Effect of Series Compensation

Series compensation is a proven technology mainly used to increase the transfer capacity of long lines and improve system stability. The effect of the series capacitor bank on one-terminal fault location algorithms is explained by referring to the faulted circuit shown at Figure 3.

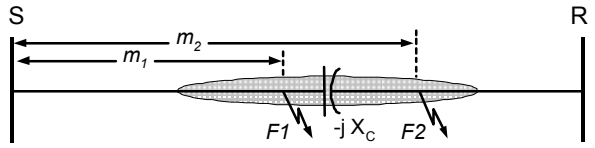

Fig. 3: One-line diagram of a three phase series compensated line considering two fault location possibilities (in front and beyond the capacitor)

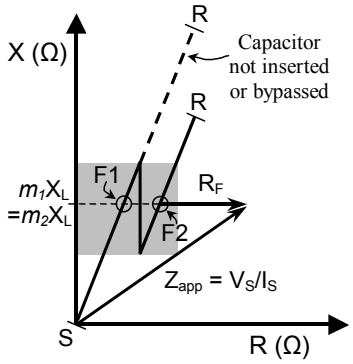

Figure 4: R-X Diagram of Series Compensated Line

The simplified circuit represents the one-line diagram of a three phase series compensated line between terminal *S* and terminal *R*. A fault *F1* is first considered at distance m_1 from terminal *S*, in front of the capacitor bank. The capacitive reactance *Xc* is compensating X_C/X_L percent of

the total inductive reactance of the line X_L (the latter is not shown for clarity purpose). The capacitor is introducing a discreet jump in the series impedance of the line that translates into a broken line in the R-X diagram as shown at Figure 4.

For analysing the effect of the capacitor on the reactance algorithm, let's assume that the error introduced by the remote-end infeed is negligible. Referring to Figure 3 and 4, it can be seen that there exists a second fault *F2* at a location m_2, beyond the capacitor bank, that may lead to the same apparent reactance as for fault *F1*. The greyed region shown at Figure 3 illustrates the locations where two results cannot be discriminated when using fundamental frequency phasors. The extent of this region is dependent on the percentage of compensation. It is proposed in [12] to compute the apparent impedance at two frequencies to discriminate between the two results. Conventional one-terminal fault location algorithms could be modified to take into account the voltage drop across the capacitor if assuming its reactance is fixed in all conditions. Such simplistic model of the capacitor bank is not valid however when considering the action of its protective devices during severe faults. For explaining the implications on fault location, a typical modern protection scheme is shown at Figure 5 [13].

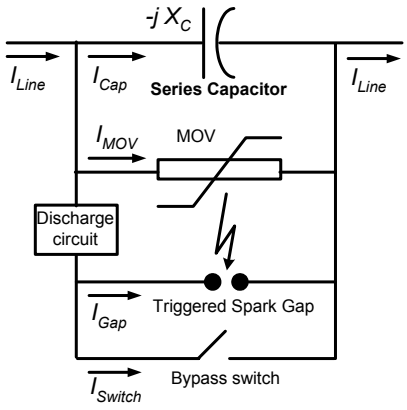

Figure 5: MOV Gap Scheme for Protecting Fixed Series Capacitor [13]

This scheme consists of metal oxide varistors (MOV), triggered spark gap and bypass switch in parallel with the capacitor. The purpose of the MOV is to protect the capacitor from overvoltage resulting from large through currents I_{Cap}. It exhibits highly non-linear V-I characteristic as shown at Figure 6 and conducts mainly when its applied voltage exceeds a threshold, thus diverting partially a current I_{MOV}. An equivalent model generally used to represent the MOV at the fundamental frequency consists of a capacitive reactance in series with a resistance, both of which being non-linear functions of the through current [14], [15].

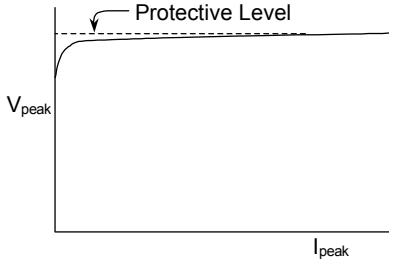

Figure 6: MOV V-I Characteristic [13]

The triggered gap and/or bypass breaker in turn are used to protect the MOV against thermal damage caused by severe faults and overload conditions. The MOV protection consists typically of Energy Absorption Monitoring, High Current Protection and Temperature Overload [13]. All these non-linear functions complicate the calculation of the voltage drop across the capacitor bank when using only local measurements.

2.4 One-Terminal Fault Location Algorithms for Series Compensated Lines

The voltage drop across the capacitor bank must be calculated using a detailed model of many non-linear elements. In spite of these difficulties, some authors have proposed one-terminal fault location algorithms for series-compensated lines [16]-[20]. In [16], the fault resistance, local and remote source impedances and equivalent electromotive forces are all assumed constant during the fault. The shunt capacitance of the line is neglected in first approximation. Also, the remote source impedance, the prefault and fault type are required before solving the equations by an iterative method. The V-I curve of the MOV is necessary and the authors suggest to accurately measure the characteristic of the installed MOV in order to remove uncertainty about the MOV parameters (the reference voltage, primarily). They extended the method for series compensated parallel lines [17] and the latter method was improved once again to avoid requiring source impedance and prefault data [18]. It is assumed that the recorded voltage and current data cover the time window when the MOVs actually operate and are not short-circuited by the gap and/or the bypass switch. This constraint supposes that the bypass time can be accurately determined. It should be noted that the assumed equivalent model of the MOV derived at the fundamental frequency is a steady-state model valid for perfect sinusoidal voltages and currents. In reality, there are many transient components, such as the decaying

DC offset and the subsynchronous resonance on the fault current, that are superposed on the steady-state component. The MOV protection is submitted to the resulting time-domain signals and its protective functions being non-linear, it seems not possible to predict accurately the bypass time when considering only a steady-state model.

In [19], three methods are investigated to compute the voltage drop across the capacitor bank using only the local current. A phasor-based deterministic Linear Model (LM), a time-domain Deterministic Differential Approach (DDA) and a time-domain Artificial Neural Network (ANN) are compared. The authors recognize the disadvantage of the LM model for estimating the bypass time of the MOV. The DDA approach also requires the detailed modeling of the capacitor bank. According to the authors, large error can result in the estimated voltage across the capacitor if the energy calculation has not been accurate for the prediction of the overload protection operation. The ANN approach doesn't provide better results. In [20], an hybrid approach combining ANN and Fuzzy Logic System (FLS) is proposed. From a practical point of view, the adoption of ANN techniques by utilities in general faces reticence when considering the considerable efforts required for the training and testing.

The above mentioned studies provide a valuable insight into the difficulties that arise when considering fault location for series compensated lines. The behaviour of the capacitor bank complicates the problem tremendously as the following comment from [21] testifies to this:

> *"However, location of fault point and protection of systems with series compensated lines is considered as one of the most difficult task for relay manufacturers and utility engineers".*

Another citation from [15] emphasizes the fault location difficulties:

> *"Fault location in series compensated lines presents, however, even bigger challenge than distance protection".*

One last comment in the discussion of [16] is as eloquent:

> *"The authors are quite intrepid to attack the problem of fault location on transmission lines equipped with series capacitors".*

In section 3 next, a brief review of some two-terminal fault location algorithms for uncompensated lines that solve the remote-end infeed problem is presented. A new two-terminal fault location algorithm that solve both the remote-end infeed and series compensation problems is then presented in section 4.

3. TWO-TERMINAL FAULT LOCATION ALGORITHMS FOR UNCOMPENSATED LINES

It was shown in the previous section the limitations of one-terminal fault location algorithms when dealing with remote-end infeed and series compensation. Two-terminal fault location algorithms for conventional uncompensated lines are treated in this section as an introduction for the next section dealing with series compensated lines. Obviously, the remote-end infeed that was causing an error with one-terminal algorithms should be eliminated with two-terminal algorithms since the remote-end current is measured.

3.1 A Review of an Old Concept

Contrary to common belief, two-terminal algorithms are not recent. In a paper published in 1950 [22], the authors are describing the principle of a method by stating first:

> *"The well known principle of the method described below for location of transient faults is based on the utilisation of the symmetrical components of the currents, voltages, and impedances and on the application of Ohm's Law to the two sections of line lying between the faults and the two ends of the line."*

The method described is worth examining because it is the basis of most two-terminal methods that have been proposed more recently [9], [23-31]. The method is recalled by referring at Figure 1. The nomenclature adopted here differs from the original paper to maintain consistency throughout this paper.

It is assumed first that the circuit at Figure 1 represents a single-phase line. The expression of the voltage drop in the two line sections *S-F* and *R-F* is obtained by applying the Ohm's Law as follows:

$$V_F = V_S - m \cdot Z_L \cdot I_S \tag{15}$$

$$V_F = V_R - (1-m) \cdot Z_L \cdot I_R \tag{16}$$

Eliminating V_F leads to an explicit equation providing the sought distance:

$$m = \frac{V_S - V_R + Z_L \cdot I_R}{Z_L \cdot (I_S + I_R)} \tag{17}$$

Equations (15-17) are general and can be applied to any decoupled symmetrical component network. The zero sequence component was chosen by the authors to locate principally phase-to-ground and double-phase-to-ground faults. Thus, Equation (17) was rewritten as follows:

$$m = \frac{V_{S0} - V_{R0} + Z_{L0} \cdot I_{R0}}{Z_{L0} \cdot (I_{S0} + I_{R0})} \tag{18}$$

The authors have adopted a graphical method to solve rapidly the complex Equation (18), obviously because the computational means were limited at that time. Equating Equation (15) and (16) and assuming that the zero sequence component is used leads to:

$$V_{S0} - m \cdot Z_{L0} \cdot I_{S0} = V_{R0} - (1-m) \cdot Z_{L0} \cdot I_{R0} = V_{F0} \qquad (19)$$

Equation (19) is expressing the voltage drop up to the fault point that is calculated from measurements at each end taken separately. It is used to plot the voltage profile along the line as shown at Figure 7. The sought distance m is found at the intersection of the two lines, which corresponds to the zero sequence voltage V_{F0} at the fault point F. It can be noticed that the zero sequence voltage attains its maximum at the fault point as expected.

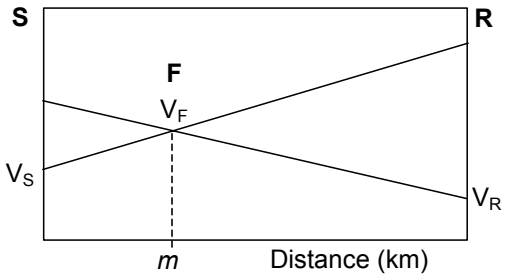

Figure 7: Simplified Two-Terminal Fault Location Graphical Method

An assembling of fast zero sequence analog ammeters and voltmeters of clamped needle type have been used to test the method in the field. The system has been put into service the 1st of January 1949 on a 220 kV line of the French transmission system. Three staged faults have been located with an error representing 3.4% of the whole length of this line 85 km long, which is remarkable for the epoch.

3.2 The Evolution of Two-Terminal Methods

Surprisingly, the *"well known principle of the method"* as stated by the authors seems to have been almost forgotten in the following years. This is probably due to the lack of digital equipment for measuring and transmitting the information from both ends and the laborious task of preparing the sheets which exhibit six axes at different scales for tracing the voltage drops. No mention of the paper nor the method is made in reviews of fault location methods in 1956 [32] and 1957 [33]. It can be noticed from these reviews that travelling-wave based methods were attracting much attention at that time. However, methods using digital voltage and current data gained considerable popularity with the development of DFRs and microprocessor relays in the '80s [5], [23], [34], [35]. Two-terminal fault location algorithms aiming to overcome the one-terminal algorithm limitations became also more interesting with the lightning progress in digital communication.

Many two-terminal fault location methods have been proposed since then [9], [23]-[29], [31], [34], [36]-[39]. It is now recognized that the positive and/or negative sequence network is a better choice than the zero sequence network because these are not influenced by the soil resistivity and they are immune to the zero sequence mutual coupling between parallel lines for ground faults [9], [24], [40]. The proposed methods differ depending on various considerations about the line model (R-L, Pi or distributed parameters), the method of solution (single step or iterative), the requirements (faulted phase selection required or not, synchronized or unsynchronized measurements), etc.

Sometimes the terms *phasor-based* and *impedance-based* are use indiscriminately in the literature to classifiy these methods. It is the present authors opinion that the term phasor-based is more general and impedance-based should be restricted to designate methods that are calculating an impedance explicitly. Most two-terminal algorithms determine the distance without calculating an impedance, such as Equation (17) which expresses a voltage ratio. A few two-terminal algorithms solving equations in the time-domain have been proposed for uncompensated lines [38], [39] and series compensated lines [21]. They seem promising because the transient natural response of the network is considered into the equations. However, high sampling rate requirement which is necessary when considering the travelling time of the waves may preclude the use of common DFRs and digital relays.

3.3 Two-terminal fault location algorithms using distributed parameter line model

It was shown in section 2 that one-terminal fault location algorithms for uncompensated lines have inherent residual error owing to the remote-end infeed. Two-terminal algorithms that overcome these limitations are briefly described next. The method proposed in [9] leads to an explicit equation for solving the fault location problem whereas in [27] an iterative method is used to account for possible synchronization error. In both cases, a distributed parameter line model is used, which provides an exact solution for lines of any length. For explaining the principle of the methods, the one-line diagram of a three-phase faulted uncompensated line is shown at Figure 8. The representation of the distributed R-L-C parameters are omitted on the diagram for clarity. It should be noticed that the currents at both ends of a healthy line section are no

longer equal each other because of the charging current of the line.

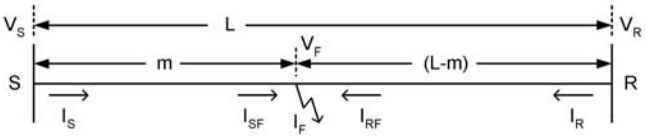

Figure 8: One-line diagram of a three-phase faulted uncompensated line

A healthy line section of length x can be represented by the Two-Port network shown at Figure 9:

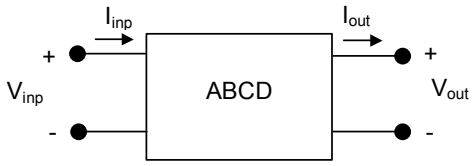

Figure 9: Two-Port Network

Considering the single-phase case first, the voltage V_{out} and current I_{out} at the output are related to the voltage V_{inp} and current I_{nip} at the input using the Two-Port equations [8]:

$$V_{out} = A(x)\, V_{inp} - B(x)\, I_{inp} \quad (20)$$
$$I_{out} = -C(x)\, V_{inp} + D(x)\, I_{inp} \quad (21)$$

Equations (20-21) can be written in matrix format:

$$\begin{bmatrix} V_{out}(x) \\ I_{out}(x) \end{bmatrix} = \begin{bmatrix} A(x) & -B(x) \\ -C(x) & D(x) \end{bmatrix} \begin{bmatrix} V_{inp} \\ I_{inp} \end{bmatrix} \quad (22)$$

For a distributed parameter line model, the Two-Port parameters are:

$$A(x) = D(x) = \cosh(\gamma x) \quad (23)$$
$$B(x) = Z_c \sinh(\gamma x) \quad (24)$$
$$C(x) = \frac{1}{Z_c} \sinh(\gamma x) \quad (25)$$

where: $\gamma = \sqrt{zy}$: propagation constant (m^{-1})

$Z_c = \sqrt{z/y}$: characteristic impedance (Ω)

$z = R' + j\omega L'$: series impedance (Ω/m)

$y = G' + j\omega C'$: shunt admittance (S/m)

Equation (20) can be used to relate the faulted voltage V_F to the measurements at each end taken separately, similar to Equations (15-16) for the R-L line model:

$$V_F = A(mL)\, V_S - B(mL)\, I_S = f_S(m) \quad (26)$$
$$V_F = A((1-m)L)\, V_R - B((1-m)L)\, I_R = f_R(m) \quad (27)$$

Equating Equations (26) and (27) eliminates the faulted voltage V_F. Rearranging and isolating m leads to an explicit equation as Equation (17) giving the sought distance [9]:

$$m = \frac{1}{\gamma} a\tanh\left(\frac{V_S + Z_c \sinh(\gamma L) I_R - \cosh(\gamma L) V_R}{Z_c I_S + Z_c \cosh(\gamma L) I_R - \sinh(\gamma L) V_R} \right) \quad (28)$$

For a multi-phase system, the transformation to modal components leads to equations such as (20-28) for each decoupled mode [9], [30], [41], [42]. Equation (28) which applies to any line length can be compared to Equation (17) which is accurate for short lines only. The method is general and it applies to continuously transposed, discretely transposed or untransposed lines, with or without parallel lines. The different variants of this method that are proposed are usually using the positive sequence component for balanced (three-phase) faults, the negative sequence component for unbalanced faults or both component in any case.

Synchronization Issues

Before using Equation (28), the measurements at terminal S and R must be accurately synchronized in order to preserve the phase relationship between the phasors from both ends with an error not exceeding a few degrees. Considering for instance that ±1 degree at 60 Hz corresponds to ±46.3 µs, it can be established that measurements referenced to GPS clocks having ±1 µs precision (0.0216 degree) satisfy largely the requirement and no correction is necessary. On the other hand, a time code that would exhibit a ±1 ms precision would represent an error of about 1/16th cycle or ±21.6 degrees. Such low accuracy synchronization is susceptible of introducing large error in the fault location estimate. It is possible however to correct a synchronization error δ between the measurements from both ends using the prefault modal components of the voltages and currents according to [9], [23]. Considering the measurements at terminal S as being the reference for the synchronous phasors, Equation (20) can be used to estimate the synchronous prefault positive sequence voltage V'_{R1pref} at the remote end from the local measurements V_{S1pref} and I_{S1pref}:

$$V'_{R1pref} = A(L)\, V_{S1pref} - B(L)\, I_{S1pref} \quad (29)$$

An estimate of the synchronization error δ for the voltages is given by the phase difference between V'_{R1pref} and the actual measurement V_{R1pref}:

$$\delta = angle(V'_{R1pref}) - angle(V_{R1pref}) \quad (30)$$

Equations (29-30) are valid for continuously transposed lines and other equations are given in [30] for untransposed and discretely transposed lines. The synchronization error is then compensated by correcting the phase of the signals at terminal *R*:

$$V_R' = V_R\, e^{j\delta} \quad (31)$$

$$I_R' = I_R\, e^{j\delta} \quad (32)$$

3.4 Improved two-terminal fault location algorithm using unsynchronized measurements

If the measurements are not precisely synchronized and the prefault data is unavailable or unreliable at one end or the other, the synchronization error cannot be determined and the fault location estimate given by Equation (28) may be inaccurate and present an imaginary component. A phase error in voltage and current phasors of ± 10º (±0.46 ms at 60 Hz) results in a fault location error of 1.5% as shown in [9]. If a time code having ± 1 ms accuracy is used for time-stamping the data for instance, the fault location error would be worst.

A method proposed in [27] also uses distributed parameter line model and provides exact steady-state solution but it is more tolerant to synchronization error. The method proceeds by taking the magnitude of Equation (26) and (27) before equating them. The distance *m* is then found iteratively when the following function attains a minimum:

$$F(m) = \left| \left| f_S(m) \right| - \left| f_R(m) \right| \right| \quad (33)$$

The method is used routinely at Hydro-Québec and it provides very accurate results. The next section addresses the much more difficult problem of locating faults for series compensated lines.

4. TWO-TERMINAL FAULT LOCATION ALGORITHMS FOR SERIES COMPENSATED LINES

One-terminal fault location algorithms present limitations when considering remote-end infeed and series compensation as explained in section 2. Some two-terminal fault location algorithms that solve the remote-end infeed problem and provide exact steady-state solution for uncompensated lines of any length were described in section 3. However, series compensation also invalidates these methods. One exception to this rule exists when the capacitor bank is located at one end of the line and the potential transformers are located on the line side [43]. Since the capacitor is then not part of the voltage drop equation, conventional fault location methods can be applied in this case. The performance of the one-terminal Takagi method [5] and a two-terminal method similar to Equation (15) are compared in [44] for such configuration.

4.1 Two-Terminal Current-Based Fault Location Method

In the recent *"IEEE Guide for Determining Fault Location on AC Transmission and Distribution Lines"* [43], no general phasor-based method is recommended for series compensated lines. A graphical current-based method is presented however for the particular case of low degree of compensation and low protection limit of the capacitor assuming a gap scheme. The method requires extensive fault studies, aiming to determine the magnitude of the currents from both ends that are expected for different fault types and fault locations. For each fault type, the two curves that are obtained (one for each end) are plotted on a *'Current magnitude'* versus *'Distance'* graph. The approach is similar to the *"Current-Distance curves"* that were presented in [45] sixty years ago for uncompensated lines. The expected accuracy was 2% to 4% owing to the authors but no field result confirmed that estimation. In [46] published a year later, a graphical fault location method based on ground current distribution is presented. The detrimental effect of resistive faults, various amount of generation and status of nearby lines on the precision of the current curve method is disclosed. In such situations, it was recommended to use ratio curves to minimize these errors. Nevertheless, it was admitted that the location of ground faults is accurate only if fault resistance is low. The same reasons explain why current-based relays doesn't make distance relays. The fault current distribution is indeed dependant on unknown and changing parameters such as the source impedances, the fault resistance and the network configuration at the very moment the fault occurs. Series compensated lines represent even larger error because in some points on the curve, there exist two fault locations that lead to the same current magnitude. Moreover, it is observed in [15] that the combination of series capacitor and MOV acts as a "fault current stabilizer", owing to the action of the MOV. The net effect is that the fault current versus fault location curve is flatter for series-compensated lines. Thus, small variation of the fault current may lead to large variation of the fault distance. The present authors are not aware of any published field results obtained using current-distance curve methods or phasor-based methods applied to series compensated lines.

4.2 New Two-Terminal Fault Location Algorithm for Series Compensated Lines

The new phasor-based fault location algorithm for series compensated lines is described by referring at Figure 10. It represents the one-line diagram of a faulted three phase series compensated line. The protective circuit of the capacitor is not illustrated for clarity. If the measurements are not synchronized, then the new method described next is applied to determine and correct the synchronization error.

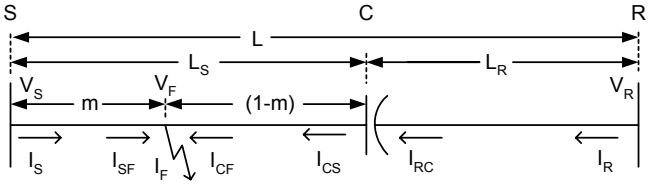

Figure 10: One-line diagram of a three phase faulted series compensated line

New Method for Synchronizing Measurements Using Prefault Data

The new method determines the synchronization error to a suitable precision using the positive sequence prefault data from both ends. The minimum requirements for using unsynchronized measurements is to have sound prefault at both ends and of course two records that correspond to the same fault. Two-Port equations similar to (29-30) could be used to calculate the positive sequence voltage at the remote-end from local positive sequence voltage and current. The voltage drop across the capacitor bank is easily taken into account in steady-state provided that the status of the capacitor and the percentage of compensation (if inserted) is known. An alternative method is proposed here which does not require any knowledge about the capacitor bank. The synchronization error δ can be determined indeed by observing at Figure 10 that the line currents I_{RC} and I_{CS} at either side of the capacitor bank are equal:

$$I_{CS1pref} = C_1(L_S)\, V_{S1pref} - D_1(L_S)\, I_{S1pref} \quad (34)$$

$$e^{j\delta} \cdot I_{RC1pref} = -C_1(L_R)\, V_{R1pref} + D_1(L_R)\, I_{R1pref} \quad (35)$$

Thus, the angle δ is simply obtained:

$$\delta = angle(-C_1(L_R)\, V_{R1pref} + D_1(L_R)\, I_{R1pref}) - angle(C_1(L_S)\, V_{S1pref} - D_1(L_S)\, I_{S1pref}) \quad (36)$$

The synchronization error is then corrected using (31-32). This synchronization method is valid irrespective of the status of the capacitor bank or the percentage of compensation. It is possible to use oscillographic records from DFRs or digital relays that don't have any time reference at all. If using such unsynchronized measurements, it is necessary however to detect the beginning of the fault to a precision of ±1/4 cycle to avoid a cycle misalignment. A mixed method in the frequency- and time-domain is presented in [47] to determine if the prefault data is sound and to detect quite precisely the beginning of a perturbation. Using appropriate signal processing for resampling the signals, it is even possible to use measurements digitized at different bit resolution, different sampling rates and different record lengths.

Performing Integrity Checks

The method described previously to synchronize the measurements allows also to perform some integrity checks. For example, the magnitude of the currents $I_{CS1pref}$ and $I_{RC1pref}$ calculated using Equation (34-35) should be similar. If the measurements are synchronized, Equation (36) could still be applied to verify if the calculated synchronization error is not exceeding acceptable limits. A large discrepancy could reveal an error with the timing, the mesurements or the line parameters. Moreover, if the capacitor status and percentage of compensation is known, some end-to-end integrity checks can be performed to detect crude error into the measurements or the line parameters by using the Two-Port equations and the voltage drop calculation across the capacitor bank.

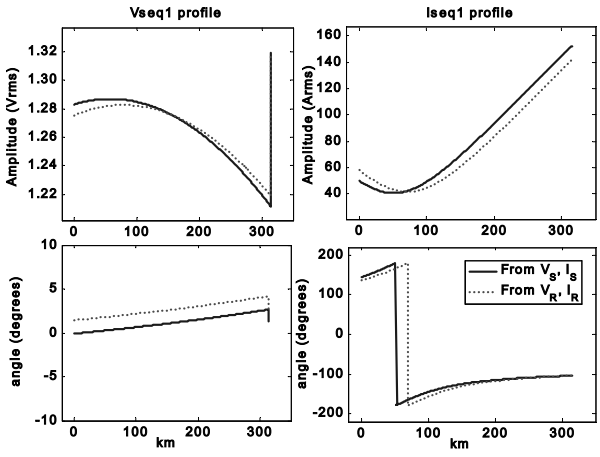

Figure 11: Positive sequence voltage and current profiles

Figure 11 illustrates the positive sequence voltage and current profiles along a 230 kV line of length 315 km. The profiles computed from V_{S1pref} and I_{S1pref} are plotted along the profiles computed from V_{R1pref} and I_{R1pref} and these should superpose exactly if perfect measurements and line parameters are used. The step in the voltage near the end of the line is due to a 73 Ohm series capacitor at the remote substation, which is taken into account. These plots highlight the non linear nature of the profiles and emphasize

the need to consider the charging current, especially with lightly loaded long lines. It can be observed that the amplitude of the current at one end of the line is about three times the current at the other end in this particular case. More integrity checks are presented in [47].

Fault Model

The principle of the method relies on the noting that the fundamental voltage across a fault, whether it is solid (metallic), arcing in free air or conducting through other medium (tree, soil, etc.), is in phase with the fundamental fault current. Thus, the fault impedance can be represented as a pure resistance R_F in the phasor domain, as it was assumed for the reactance-type algorithms. This fault model is fairly realistic in spite of the square-wave shape of the voltage during arcing fault [48]. Voltage and current measurements of a real fault which occurred in a 735 kV substation is shown at Figure 12 to illustrate this behaviour.

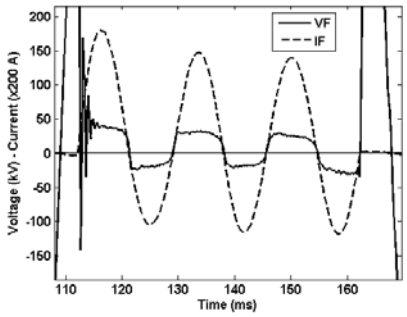

Figure 12: Faulted voltage and current measurements (735 kV sectionalizer arm fallen on a CCVT)

Single-Phase Case

The new two-terminal algorithm avoids calculating the voltage drop across the capacitor bank. Thus, the complex modeling of the non linear protective elements is unnecessary and not any related parameter must be provided. The new algorithm is explained by referring to Figure 10 and considering the circuit is single phase at first. The fault is first assumed to be located on the line section *S-C* of length L_S. The distance m (in percent of L_S) from terminal *S* is determined iteratively by finding the location x in the interval [0, Ls] where V_F and I_F are in phase. The derivation of the equations next is aiming to express V_F and I_F in terms of the distance m and the measurements V_S, I_S, V_R and I_R.

The total fault current I_F is first expressed as the sum of the contributions I_{SF} and I_{CF}:

$$I_F = I_{SF} + I_{CF} \tag{37}$$

Next, the voltage V_F and the current I_{SF} are determined by the Two-Port equations using the distributed parameter line model (20-21):

$$V_F = \cosh(\gamma m L_S) V_S - Z_c \sinh(\gamma m L_S)\, I_S \tag{38}$$

$$I_{SF} = -Z_C^{-1} \sinh(\gamma m L_S)\, V_S + \cosh(\gamma m L_S)\, I_S \tag{39}$$

Similarly, the current I_{RC} can be determined from V_R and I_R:

$$I_{RC} = -Z_C^{-1} \sinh(\gamma L_R)\, V_R + \cosh(\gamma L_R)\, I_R \tag{40}$$

By applying the Kirchoff's Current Law (KCL) to the series capacitors circuit at Figure 5, it should be recognized that the line current I_{Line} passes through the capacitor bank unchanged, irrespective of its division between the parallel branches when the protective elements conduct. Thus, the current I_{RC} and I_{CS} on each side of the capacitor bank at Figure 10 are equal:

$$I_{CS} = I_{RC} \tag{41}$$

Next, the Two-Port Equation (21) is rearranged by isolating the input current:

$$I_{inp} = (C(x)\, V_{inp} + I_{out}) / D(x) \tag{42}$$

By appropriate substitutions, the current I_{CF} can be expressed in terms of V_F and I_{CS}:

$$I_{CF} = (I_{CS} - Z_C^{-1} \sinh(\gamma(1-m)L_S)\, V_F) / \cosh(\gamma(1-m)L_S) \tag{43}$$

By substituting (38) in (43), then (40) and (43) in (37), the voltage V_F and current I_F are finally expressed in the appropriate form. The fault impedance Z_F is then simply the ratio:

$$Z_F = V_F / I_F \tag{44}$$

The solution m corresponds to the location where Z_F has minimum reactance, which is solved iteratively by minimizing the following objective function:

$$F(m) = \text{abs}(\text{imag}\{Z_F\}) \tag{45}$$

The same reasoning is applied to line section *R-C* of length L_R by permuting the indices *S* and *R*. Most of the time, only one of the two line sections presents a location exhibiting a negligible fault reactance and that result must be kept as the right answer. If both line sections exhibit a small reactive component, the location presenting the lowest fault resistance R_F is kept, where R_F is simply the real part of the fault impedance:

$$R_F = \text{Real}\{Z_F\} \tag{46}$$

The knowledge of the fault resistance is also useful to estimate the cause of the fault.

Three-Phase Case

The above described method can be extended to three phase systems, whether the line is transposed or untransposed, with or without parallel lines, by decoupling the Two-Port equations with a modal transformation matrix [9], [30], [41], [42]. At the fault point, the modal components are transformed back to phase quantities and the expression of the fault impedance depends on the fault type. For example, for a phase-a-to-ground fault, Equation (44) becomes:

$$Z_F = V_{Fa} / I_{Fa} \tag{47}$$

The algorithm provides an exact steady-state solution. According to the classification of the errors in [49], the remaining errors come from the transducers (CT, CCVT, inputs), the model approximations and the measurement (phasor estimation principally). The algorithm is not dependent on external parameters such as the source impedances or the current distribution factors. It is not influenced by the fault resistance and it takes into account the distributed nature of the shunt capacitance of long lines. The modeling of the capacitor bank is avoided and even its capacitance or its status is not required. It should be noticed however that the principle doesn't apply to multiple capacitor banks on a single line.

5. IMPLEMENTATION AND FIELD EXPERIENCE AT HYDRO-QUÉBEC

5.1 Characteristics of the Hydro-Québec Network

Hydro-Québec transmission system covers vast territory. It consists of over 32,000 km of transmission lines operating between 69 kV and 765 kV as detailed in Table 1. The bulk network illustrated at Figure 13 consists of 11,422 km of 735 kV lines, of which about 8,000 km are series compensated [50]. Some lines cover 400 km mostly in uninhabited region and cold climate in winter. These characteristics explain the high interest of Hydro-Québec for accurate fault location algorithms.

TABLE I: Hydro-Québec transmission system

Voltage	Lines (km)
735-765 kV	11 422
450 kV DC	1 218
315 kV	5 068
230 kV	2 976
161 kV	1 875
120 kV	6 600
69- kV	3 385
Total	**32 544**

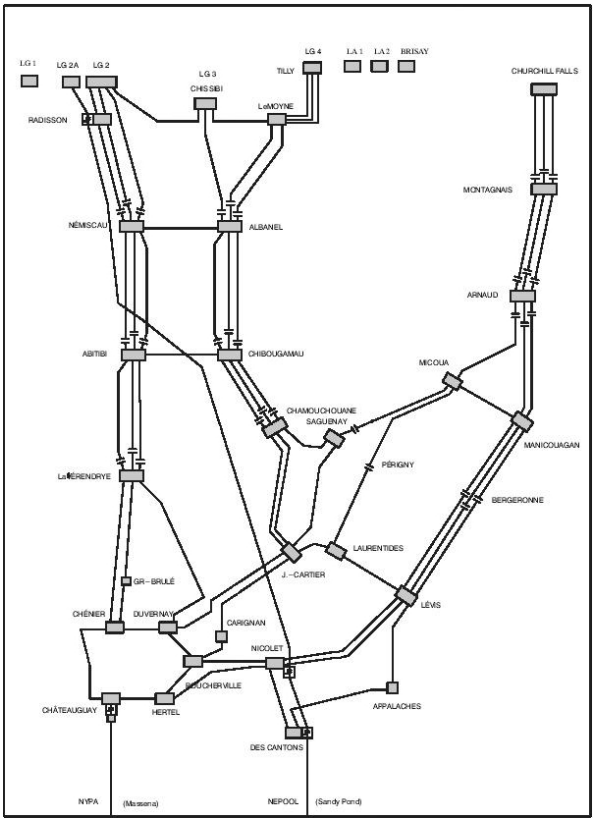

Figure 13: Hydro-Québec 735 kV Bulk Network

5.2 Automated Fault Location System Overview

Hydro-Québec has undertaken a vast program to replace its light beam oscillographs by digital fault recorders in the beginning of the nineties. Today, about 200 DFRs are installed and a majority of them are used to monitor near 600 ends of transmission lines. This technology shift permitted the automatic transmission of the records to a central location and their computerized processing. The time to transmit the records to the central office has been reduced from days, with the old photo-sensitive paper rolls, to a few minutes with the new digital format over telecommunication links. The Figure 14 illustrates the architecture of the automated fault analysis and fault location system. When a DFR is triggered by a fault on a transmission line, its record is sent automatically to the central server for processing by the fault location algorithms. The system also uses commercial travelling wave fault locators that are installed in pairs at each end of about twenty lines judged more important. Hydro-Québec also uses a lightning positioning system called *ORAGELECT*® to aid in the localization of faults caused by lightning.

Once the results are obtained, an email is sent to the concerned employees which contains the following information:

- Line number
- Date and time of breaker opening command provided by Sequence of Event Recorders (SERs)
- Fault location (km ± km and no. tower)
- Fault type, fault duration and fault resistance
- Fault location provided by ORAGELECT lightning positioning system if applicable and Travelling-Wave Fault Locator if available
- Prevailing whether conditions in the vicinity of the line (temperature, wind speed and direction, precipitations, etc.) from nearest whether station
- Ice monitoring system data

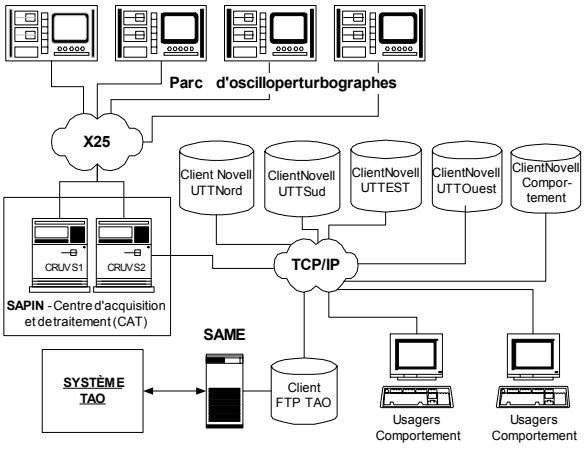

Figure 14 Overall system architecture

5.3 Hydro-Québec's Field Experience

The new two-terminal fault location algorithm for series compensated lines as developed by one of the authors has been in use for several years and has proven very satisfactory. To establish the performance of the algorithm for real faults, the following error calculation is used:

$$error = (m_{est} - m_{actual}) / L \quad (48)$$

where: m_{est} is the distance estimated by the algorithm

m_{actual} is the distance determined by the best method available in the following order: on-the-spot recognition (Visual), Travelling-Wave Fault Locator (TW) or ORAGELECT (LPS).

The excellent accuracy obtained with travelling wave fault locators with the pairing arrangement is usually within ±1 tower. The accuracy of ORAGELECT depends on the position of the thunderbolt relative to the antennas and is typically in the order of 0.4 to 4 km. Table II presents the performance of the new algorithm. Figure 15 shows the sorted errors in descending order.

5.4 Zero Sequence Impedance Field Validation

Among the results shown at Figure 15, one exhibits an error (9.4%) which exceeds what should be expected. The integrity checks that were performed using the prefault measurements shown no anomaly. These tests gave confidence that the voltage and current measurements at both ends were correct and positive sequence impedance of the line was consistent. Some doubts were then expressed about the zero sequence impedance Z_{L0} of the line. Trials and errors showed that the Z_{L0} parameter should be 25% higher than the calculated theoretical value in order to obtain an exact fault location. Such a high value corresponded to a soil resistivity of 2500 Ωm, which is far from the default value of 100 Ωm that was used in the calculation of Z_{L0}. It is a common practice recommended in many textbooks to use a value of 100 Ωm when the soil resistivity is unknown. The related fault occurred in the beginning of year 2006 and it was decided to perform field measurements at the next maintenance period scheduled for August 2006. The zero sequence impedance that was measured last month corresponded exactly to what has been predicted.

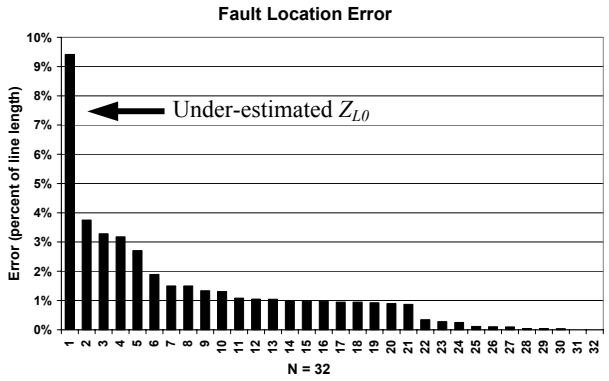

Figure 15: Error distribution

6. SUMMARY

A new fault location algorithm for series compensated lines has been presented. It uses unsynchronized measurements at both ends of the line and a new method was proposed to correct the synchronization error using the prefault data. The derivation of the equations shows that

there is no algorithmic error in steady-state. The algorithm takes into account the distributed nature of the shunt capacitance and consequently, it is suitable even for the longest EHV transmission lines. Moreover, it is insensitive to fault resistance and no assumption is made on external parameters such as the source impedances or the current distribution factors. The modeling of the capacitor and its related protection is completely avoided. Performance was evaluated using real faults that occurred on Hydro-Québec transmission lines, located by different sources. The results show an rms error of about 1.5% of line length, with an expected maximum of 4%. In one case, a 9.4% error could be attributed to a wrong zero sequence impedance estimation that was confirmed by field measurements.

7. REFERENCES

[1] U.S.-Canada Power System Outage Task Force, "Final Report on the August 14, 2003 Blackout in the United States and Canada: Causes and Recommendations", April 2004.

[2] J. F. HAUER, J. E. DAGLE, "Review of Recent Reliability Issues and System Events", CERTS, August 30, 1999.

[3] W. A. LEWIS, L. S. TIPPETT, "Fundamental Basis for Distance Relaying on 3-Phase Systems", *AIEE Trans.*, Vol. 66, pp. 694-709, 1947.

[4] K. SRINIVASAN, A. ST-JACQUES, "A New Fault Location Algorithm for Radial Transmission Lines with Loads", *IEEE Trans. on Power Delivery*, Vol. 4, No. 3, pp. 1676-1682, July 1989.

[5] T. TAKAGI, Y. YAMAKOSHI, M. YAMAURA, R. KONDOU, T. MATSUSHIMA, "Development of a New Type Fault Locator Using One-Terminal Voltage and Current Data", *IEEE Trans. on Power Apparatus and Systems*, Vol. PAS-101, No.8, pp. 2892-2898, August 1982.

[6] M. T. SANT, Y. G. PAITHANKAR, "Online Digital Fault Locator for Overhead Transmission Line", *Proc. IEE*, Vol. 126, No. 11, pp. 1181-1185, Nov. 1979.

[7] L. ERIKSSON, M. M. SAHA, G. D. ROCKEFELLER, "An Accurate Fault Locator with Compensation for Apparent Reactance in the Fault Resistance Resulting from Remote-End Infeed", *IEEE Trans. on Power Apparatus and Systems*, Vol. PAS-104, No. 2, pp. 424-436, Feb. 1985.

Table II: Algorithm performance for real faults (distance in km)

No	kV	Type	L	L_S	Visual	TW	LPS	m_{est}	err%	Cause
1	735	BCN	374.6	134.6	n/av	n/av	202.1	196.5	1.5	Lightning
2	735	AN	379.8	137.8	173.5	n/av	n/ap	173.3	0.0	Defective insulator
3	220	BCN	314.1	314.1	n/av	187.4	n/av	184.0	1.1	Lightning on double circuit line
4	220	BCN	314.1	314.1	n/av	187.4	n/av	184.1	1.1	Lightning on double circuit line
5	735	CN	275.1	275.1	266.6	n/av	n/ap	266.9	0.1	Ruptured guy wire
6	735	CN	374.6	134.6	325.3	n/av	n/ap	320.3	1.3	Tree beneath line
7	735	CN	374.6	134.6	325.3	n/av	n/ap	320.4	1.3	Tree beneath line
8	735	CN	374.6	134.6	325.3	n/av	n/ap	318.2	1.9	Burning tree beneath line
9	735	AN	411.5	224.2	n/av	n/av	214.7	211.0	0.9	Lightning
10	220	BCN	314.1	314.1	n/av	201.0	n/av	205.7	1.5	Lightning on double circuit line
11	220	ABC	314.1	314.1	n/av	201.2	n/av	209.7	2.7	Lightning on double circuit line
12	735	BN	378.1	137.8	n/av	n/av	354.9	354.5	0.1	Lightning
13	735	BN	411.5	187.23	295.0	n/av	n/ap	291.0	1.0	Ground wire touching phase conductor (freezing rain)
14	735	BN	411.5	187.23	295.0	n/av	n/ap	291.2	0.9	Ground wire touching phase conductor (freezing rain)
15	735	BN	411.5	187.23	295.0	n/av	n/ap	291.0	1.0	Ground wire touching phase conductor (freezing rain)
16	735	BN	411.5	187.23	295.0	n/av	n/ap	291.1	0.9	Ground wire touching phase conductor (freezing rain)
17	735	BN	411.5	187.23	295.0	n/av	n/ap	291.1	0.9	Ground wire touching phase conductor (freezing rain)
18	735	BN	411.5	187.23	295.0	n/av	n/ap	290.9	1.0	Ground wire touching phase conductor (freezing rain)
19	735	ABN	167.9	0.0	n/av	n/av	73.6	79.9	3.8	Lightning
20	735	AN	251.6	251.6	143.7	n/av	n/ap	167.4	9.4	Broken "U" bolt
21	315	BC	184.5	139.8	11.0	n/av	n/ap	11.0	0.0	Conductor galloping
22	315	AB	184.5	139.8	10.0	n/av	n/ap	10.0	0.0	Conductor galloping
23	735	AN	378.1	137.8	378.1	n/av	n/ap	377.0	0.3	Sectionalizer
24	735	AN	378.1	137.8	378.1	n/av	n/ap	377.1	0.3	Sectionalizer
25	735	CAN	411.5	224.2	192.0	n/av	192.3	190.6	0.3	Damaged insulators (lightning)
26	735	BN	270.7	270.7	0.0	n/av	n/ap	0.3	0.1	Defective shunt inductance
27	735	AN	378.1	240.26	194.7	n/av	n/ap	207.1	3.3	Ground wire too close to conductor (freezing rain)
28	735	AN	378.1	240.26	194.7	n/av	n/ap	206.7	3.2	Ground wire too close to conductor (freezing rain)
29	735	CN	222.8	0.1	0.0	n/av	n/ap	0.1	0.0	CT of shunt inductance
30	735	BN	275.1	275.1	275.1	n/av	n/ap	275.0	0.0	Aux. contact of shunt inductor breaker exploded
31	735	CN	230.1	230.1	0.0	n/av	n/ap	2.4	1.0	Defective Shunt Inductance
32	735	CN	230.1	230.1	n/av	n/av	0.1	2.1	0.9	Lightning

*n/ap: not applicable, n/av: not available

[8] J. D. GLOVER, M. S. SARMA, "Power System Analysis and Design", 3rd ed., Brooks/Cole, Thompson Learning, 2002.

[9] A. T. JOHNS, S. JAMALI, "Accurate Fault Location Technique for Power Transmission Lines", *Proc. IEE of Generation, Transmission and Distribution*, Vol. 137, Pt. C, No. 6, pp. 395-402, Nov. 1990.

[10] S. E. WESTLIN, J.A. BUBENKO, "Newton-Raphson Technique Applied to the Fault Location Problem", *IEEE PES Summer Meeting*, Portland, OR, Paper A 76 334-3, July 1976.

[11] M. T. SANT, Y. G. PAITHANKAR, "Fault Locator for Long EHV Transmission Lines", *Electric Power Systems Research*, Vol. 6, pp. 305-310, 1983.

[12] D. NOVOSEL, A. PHADKE, M. M. SAHA, S. LINDAHL, "Problems and Solutions for Microprocessor Protection of Series Compensated Lines", *Proc. IEE of 6th Intl. Conf. on Development in Power System Protection*, Nottingham, UK, pp. 18-23, March 1997.

[13] A. F. ELNEWEIHI (CHAIRMAN), "Series Capacitor Bank Protection", IEEE PSRC WG K13 Special Publication, IEEE Cat. No. 98-TP-126-0, 1998.

[14] D. L. GOLDSWORTHY, "A Linearized Model for MOV-Protected Series Capacitors", *IEEE Trans. on Power Systems*, Vol. 2, No. 4, pp. 953-958, Nov. 1987.

[15] B. KASZTENNY, "Distance Protection of Series Compensated Lines – Problems and Solutions", *28th Annual Western Protective Relay Conf.*, Spokane, WA, October 22-25, 2001.

[16] M. M. SAHA, J. IZYKOWSKI, E. ROSOLOWSKI, B. KASZTENNY, "A new accurate fault locating algorithm for series-compensated lines", *IEEE Trans. on Power Delivery*, Vol. 14, No. 3, pp 789-797, July 1999

[17] M. M. SAHA, K. WIKSTRÖM, J. IZYKOWSKI, E. ROSOLOWSKI, "Fault Location in Uncompensated and Series-Compensated Parallel Lines", *IEEE/PES Winter Meeting 2000*, IEEE, Vol. 4, pp 2431-2436, 2000.

[18] M. M. SAHA, K. WIKSTRÖM, J. IZYKOWSKI, E. ROSOLOWSKI, "New Concept for Fault Location in Series-Compensated Parallel Lines", *PES Winter Meeting 2001*, IEEE, Vol. 2, pp 769-774, 2001.

[19] D. NOVOSEL, B. BACHMANN, D. HART, Y. HU, M. M. SAHA, "Algorithms for Locating Faults on Series Compensated Lines Using Neural Networks and Deterministic Methods", *IEEE Trans. on Power Delivery*, Vol. 11, No. 4, October 1996.

[20] M. JOORABIAN, R. K. AGGARAWAL, "An Accurate Fault Location Technique for Transmission Line Using Artificial Neural Network", *30th Universities Power Engineering Conference*, UPEC '95, Vol. 2, pp. 773-776, 1995.

[21] J. SADEH, N. HADJSAID, A. M. RANJBAR, R. FEUILLET, "Accurate Fault Location Algorithm for Series Compensated Transmission Lines", *IEEE Trans. on Power Delivery*, Vol. 15, No. 3, July 2000.

[22] L. CABANES, J. RAIMBAULT, P. REVOL, CH. DIETSH, P. DEVILAINE, LANOE, M. REGENT, L. ROCHE, "Practicals Results with New Equipment for Locating Transient Faults and Some Results of Slow Reclosure and Automatic Tie Line Re-Connexion", *13th Meeting of the Intl. Conf. on Large Electric Systems (CIGRE)*, Vol. III, No. 341, 1950.

[23] E. O. SCHWEITZER III, "Evaluation and Development of Transmission Line Fault-Locating Techniques Which Use Sinusoidal Steady-State Information", *Ninth Annual Western Protective Relay Conference*, Spokane, Washington, Oct. 26-28, 1982.

[24] W. A. ELMORE, "Zero Sequence Mutual Effects on Ground Distance Relays and Fault Locators", *19th Annual Western Protective Relay Conf.*, Spokane, WA, October-20-22, 1992.

[25] G. KIESSLING, S. SCHWABE, J. HOLBACH, "Power System Fault Analysis using Fault Reporting Data of Numerical Relays", *8th Annual Fault and Disturbance Analysis Conf.*, Atlanta, GA, April 25-26, 2005.

[26] D. A. TZIOUVARAS, J. B. ROBERTS, G. BENMOUYAL, "New Multi-Ended Fault Location Design for Two- or Three-Terminal Lines", *Proc. IEE of 7th Intl. Conf. on Developments in Power System Protection*, pp. 395-398, April 9-12, 2001.

[27] C. FECTEAU, D. LAROSE, C. DEGUIRE, "Nouveaux algorithmes de localisation de défauts et expérience sur le réseau de transport d'Hydro-Québec" (in French), *CIGRE Study Committee B5 Colloquium*, Sydney, Australia, 30 Sept.-1 Oct., 2003.

[28] D. NOVOSEL, D. G. HART, E. UDREN, J. GARITTY, "Unsynchronized Two-Terminal Fault Location Estimation", *IEEE Trans. on Power Delivery*, Vol. 11, No. 1, pp. 130-138, Jan. 1996.

[29] A. A. GIRGIS, D. G. HART, W. L. PETERSON, "A New Fault Location Technique for Two- and Three-Terminal Lines", *IEEE Trans. on Power Delivery*, Vol. 7, No. 1, Janvier 1992.

[30] C. E. DE MORAIS PEREIRA, L. C. ZANETTA, "Optimization Algorithm for Fault Location in Transmission Lines Considering Current Transformers Saturation", IEEE Trans. on Power Delivery, Vol. 20, No. 2, pp. 603-608, April 2005.

[31] J. IZYKOWSKI, R. MOLAG, E. ROSOLOWSKI, M. M. SAHA, "Accurate Location of Faults on Power Transmission Lines With Use of Two-End Unsynchronized Measurements", *IEEE Trans. on Power Delivery*, Vol. 21, No. 2, April 2006.

[32] AIEE COMMITTEE REPORT, "Bibliography and Summary of Fault Location Methods", *AIEE Transactions*, Vol. 74, Pt. III, pp. 1423-28, Feb. 1956.

[33] T. W. STRINGFIELD, D. J. MARIHART, R. F. STEVENS, "Fault Location Methods for Overhead Lines", *AIEE Trans. on Power Apparatus and Systems*, Pt. III, Vol. 76, pp 518-530, August 1957.

[34] G. ZIEGLER, "Fault Location in H.V. Power Systems", *Proc. IFAC Symposium on Automatic Control in Power Generation, Distribution and Protection*, Pretoria, South Africa, pp. 121-129, Sept. 1980.

[35] E. O. Schweitzer III, J. K. Jachinowski, "A Prototype Microprocessor-based System for Transmission Line Protection and Monitoring", *Eight Annual Western Protective Relay Conference*, Spokane, WA, October 1981.

[36] M. S. SACHDEV, R. AGARWAL, "A Technique for Estimating Transmission Line Fault Locations from Digital Impedance Relay Measurements", *IEEE Trans. on Power Delivery*, Vol. 3, No. 1, Jan. 1988.

[37] D. J. LAWRENCE, L. Z. CABEZA, L. T. HOCHBERG, "Development of an Advanced Transmission Line Fault

Location System. Part II: Algorithm Development and Simulation", *IEEE Trans. on Power Delivery*, Vol. 7, No. 4, pp. 1972-1983, Oct. 1992.

[38] S.M. MCKENNA, D. HAMAI, M. KEZUNOVIC, A. GOPALAKRISHNAN, "Transmission Line Modeling Requirements for Testing New Fault Location Algorithms Using Digital Simulators", *Second Intl. Conf. on Digital Power System Simulators – ICDS '97*, Montreal, Quebec, Canada, pp. 63-69, 1997.

[39] M. KEZUNOVIC, B. PERUNICIC, "Synchronized Sampling Improves Fault Location", *IEEE Computer Applications in Power*, Vol. 8, No. 2, pp. 30-33, April 1995.

[40] R. C. Bartz, E. O. Schweitzer III, "Field Experience With Fault Locating Relays", 39th Annual Conf. for Protective Relay Engineers, Texas A&M University, April 14-16, 1986.

[41] L. M. WEDEPOHL, "Application of Matrix Methods to the Solution of Travelling-Wave Phenomena in Polyphase Systems", *Proc. IEE*, Vol. 110, No. 12, pp. 2200-2212, Dec. 1963.

[42] H. DOMMEL, "Digital Computer Solution of Electromagnetic Transient in Single and Multi-Phase Networks", *IEEE Trans. on Power Apparatus and Systems*, Vol. PAS-98, No. 4, pp. 388-399, April 1969.

[43] K. ZIMMERMAN (CHAIRMAN), "IEEE Guide for Determining Fault Location on AC Transmission and Distribution Lines", IEEE Std C37.114-2004, 8 June 2005.

[44] T. MAEKAWA, Y. OBATA, M. YAMAURA, Y. KUROSAWA, H. TAKANI, "Fault Location for Series Compensated Parallel Lines", *Transmission and Distribution Conf. and Exibition 2002*, Asia Pacific, IEEE/PES, Vol. 2, 2002, pp 824-829, 2002.

[45] C. S. ROADHOUSE, O. R. HANTLA, "Fault Current-Distance Curves Help Locate Transmission Trouble", *Electrical World*, Vol. 123, No. 13, pp. 60-61, March 31, 1945.

[46] H. P. DUPUIS, W. E. JACOBS, "Fault Location and Relay Peformance Analysis by Automatic Oscillographs", *AIEE Trans. (Electrical Engineering)*, Vol. 65, pp. 442-46, June 1946.

[47] C. FECTEAU, D. LAROSE, R. BÉGIN, J.-G. LACHANCE, "Daily Integrity Checks Using Automated DFR's Records Analysis", *8th Annual Fault and Disturbance Analysis Conf.*, Atlanta, GA, April 25-26, 2005.

[48] M. B. Djuric, V. V. Terzija, "A New Approach to the Arcing Faults Detection for Fast Autoreclosure in Transmission Systems", IEEE Trans. on Power Delivery, Vol. 10, No. 4, pp 1793-98, Oct. 1995.

[49] A. G. PHADKE, M. A. XAVIER, "Limits to Fault Location Accuracy", *Fault and Distribution Conf.*, College Station, TX, April 14-16, 1993

[50] C. GAGNON, P. GRAVEL, "Extensive Evaluation of High Performance Protection Relays for the Hydro-Québec Series Compensated Network", *IEEE Trans. on Power Delivery*, Vol. 9, No. 4, pp. 1799-1811, Oct. 1994.

8. ACKNOWLEDGMENT

The author gratefully acknowledge the contributions of Denis Larose, Raymond Bégin and Jean-Guy Lachance from the Control and Protection Department of TransÉnergie, Hydro-Québec. They must be credited for maintaining databases of fault records and also for having automated the fault location process.

9. BIOGRAPHY

Claude Fecteau was born in Montreal, Canada, in 1963. He obtained his B.A.Sc. and M.A.Sc. degrees in electrical engineering from École Polytechnique, Université de Montréal, in 1986 and 1989 respectively. His Master thesis described one of the first operational PC-based transient waveform playback system for testing protective relays. He joined Hydro-Québec in 1989 as a research engineer at the IREQ research institute where he continued the development of the relay test system known as "SERA-NewWave PC-playback system". He also developed the software of a digital fault recorder and a graphical package. He invented new fault location algorithms, which are being used extensively at Hydro-Québec. His main interests are protection, fault location, signal processing and reliability. He is a member of the IEEE Power Engineering Society and Standard Association. Email: fecteau.claude@ireq.ca